A Section 508–conformant HTML version of this article is available at https://doi.org/10.1289/EHP14984.

Evaluating Metabolic Signatures in the Serum of South Korean Patients with Humidifier Disinfectant–Associated Lung Injury Identified through Untargeted Metabolomics

Jinwoo Kim,[1] *Mi-Jin Kang,*[2] *So-Yeon Lee,*[2,3] *Sang-Bum Hong,*[2,4] *Ho Cheol Kim,*[2,4] *Myung Hee Nam,*[1*] *and Soo-Jong Hong*[2,3*]

[1]Metropolitan Seoul Center, Korea Basic Science Institute (KBSI), Seoul, South Korea
[2]Humidifier Disinfectant Health Center, Asan Medical Center, Seoul, South Korea
[3]Department of Pediatrics, Childhood Respiratory and Allergy Center, Asan Medical Center, University of Ulsan College of Medicine, Seoul, South Korea
[4]Department of Pulmonary and Critical Care Medicine, Asan Medical Center, University of Ulsan College of Medicine, Seoul, South Korea

Background: The South Korean humidifier disinfectant–associated lung injury case was one of the worst disasters involving household chemical products, resulting in over 5,800 casualties. Despite the strong association between lung injury and humidifier disinfectants, the underlying pathogenic mechanisms remain unclear.

Objectives: We investigated patients with humidifier disinfectant–associated lung injury to identify key metabolic signatures, aiming to gain insights into the underlying pathogenic mechanisms based on the characteristics of these metabolites.

Methods: We employed untargeted metabolomics to assess the differential enrichment of plasma metabolites in 80 South Korean children with lung injuries caused by exposure to humidifier disinfectant containing polyhexamethylene guanidine. The key metabolites identified were subsequently validated in an independent cohort of 132 South Korean adults.

Results: In the plasma of patients with humidifier disinfectant–associated lung injuries, we observed significantly higher levels of oxidized lipids in comparison with healthy controls, with these levels negatively correlating with lung function. These metabolic signatures differentiated humidifier disinfectant–associated lung injury from other respiratory diseases in children, such as asthma and bronchiolitis obliterans. The 47 key metabolites identified in children were validated in an independent adult cohort. Furthermore, the classification performance of these metabolic signatures for humidifier disinfectant–associated lung injury achieved an accuracy of 0.97, a precision of 0.95, an F1 score of 0.97, and a recall of 1.00.

Discussion: These findings suggest a connection between humidifier disinfectant–associated lung injury and oxidative stress-induced lipid peroxidation. The oxidative stress signatures provide valuable insights into the underlying pathogenesis of humidifier disinfectant–associated lung injury and may serve as potential targets for biomarker development. https://doi.org/10.1289/EHP14984

Introduction

In 2011, a series of unknown respiratory illnesses with fatal lung injuries emerged in South Korea, particularly affecting children[1] and pregnant women.[1,2] An investigation led by the government revealed a link between affected individuals and the use of specific humidifier disinfectant products.[3–7] Humidifier disinfectant–associated lung injury (HDLI) is marked by severe, irreversible lung damage,[8,9] fibrosis,[9] pulmonary inflammation,[8,9] and airway damage.[8,9] According to the Korea Environmental Industry & Technology Institute (KEITI), a total of 5,810 cases of HDLI, including 1,312 deaths, have been officially reported as of October 2024. Before the government announced a recall of all humidifier disinfectant products in 2011, ∼10 million units had been sold.[10] Considering the scale of these sales, a significant portion of the population may have been exposed to these toxic substances, potentially resulting in far more victims than currently reported. One study estimates that ∼8.94 million individuals may have been exposed to these toxic humidifier disinfectants, with 950,000 likely experiencing adverse health events.[11] This incident stands as one of the most tragic environmental catastrophes in South Korea's history.

Further investigations revealed that the humidifier disinfectants associated with HDLI contained additional toxic molecules, including polyhexamethylene guanidine (PHMG),[12] chloromethylisothiazolinone (CMIT),[13] methylisothiazolinone (MIT),[13] and *n*-alkyldimethylbenzylammonium chloride (BKC).[14] A growing body of evidence from *in vitro*, *in vivo*, and epidemiological studies indicates that exposure to these toxic chemicals results in cell apoptosis (*in vitro*),[15,16] inflammation (*in vivo* rat model),[17] and pulmonary fibrosis (*in vitro* and *in vivo*; rat model),[16,17] ultimately resulting in death (*in vivo*; mouse model).[18] Previous studies[14,19] have demonstrated a strong association between humidifier disinfectants and severe lung injury; however, the precise mechanism by which these toxic chemicals lead to lung damage and chronic inflammation in humans remains poorly understood. Symptoms linked to HDLI, such as coughing, shortness of breath, tachypnea, and pulmonary fibrosis, are not specific to this condition,[20] making it difficult to differentiate it from other respiratory diseases. Although diagnostic criteria for HDLI are based on clinical, pathological, and radiological characteristics,[20] identifying unique features that differentiate HDLI from other lung diseases is imperative. Such differentiation not only aids in diagnosis but also provides a foundation for uncovering the underlying pathogenic mechanisms.

In this study, we aimed to identify the metabolic signatures associated with HDLI by using untargeted metabolomics to

*These two corresponding authors contributed equally to the work.
Address correspondence to Soo-Jong Hong, Department of Pediatrics, Childhood Respiratory and Allergy Center, Humidifier Disinfectant Health Center, Asan Medical Center, University of Ulsan College of Medicine, Seoul, South Korea. Email: sjhong@amc.seoul.kr. And, Myung Hee Nam, Metropolitan Seoul Center, KBSI, Seoul 02841, South Korea. Email: nammh@kbsi.re.kr

Supplemental Material is available online (https://doi.org/10.1289/EHP14984).
The authors declare they have nothing to disclose.

Received 14 March 2024; Revised 15 April 2025; Accepted 16 April 2025; Published 23 May 2025.

Table 1. Characteristics of children by HDLI group in the physical health monitoring program (Asan Medical Center, South Korea, 2014–2016, $n = 80$).

	Control ($n = 20$)	Unlikely ($n = 20$)		Probable ($n = 20$)			Definite ($n = 20$)		
Children	Mean ± SD	Mean ± SD	p^*	Mean ± SD	p^*	$p^\dagger$	Mean ± SD	p^*	$p^\dagger$
Age (y)	7.20 ± 0.41	9.05 ± 3.71	0.176	9.75 ± 2.84	0.001	0.531	6.90 ± 2.05	0.117	0.086
Sex									
Male	11	11	—	9	—	—	12	—	—
Female	9	9	—	11	—	—	8	—	—
FVC (%)	94.41 ± 11.14	102.32 ± 13.37	0.047	82.60 ± 13.32	0.002	<0.001	88.75 ± 16.73	0.216	0.013
FEV_1 (%)	94.11 ± 12.39	97.53 ± 28.30	0.386	80.55 ± 13.38	0.001	0.001	90.40 ± 19.41	0.404	0.156
FEV_1/FVC (%)	89.23 ± 4.35	89.68 ± 5.85	0.915	90.30 ± 5.70	0.38	0.612	91.20 ± 5.33	0.213	0.455
cDLCO (%)	ND	78.53 ± 13.29	—	70.75 ± 10.89	—	0.01	71.85 ± 16.39	—	0.094
Airborne HD concentration ($\mu g/m^3$)	NA	98.55 ± 58.58	—	102.91 ± 75.91	—	0.914	113.78 ± 63.98	—	0.43
Total duration of HD use (h)	NA	4,695.00 ± 3,697.52	—	5,283.60 ± 9,334.19	—	0.516	3,810.06 ± 4,333.94	—	0.318

Note: Data are shown as the mean ± SD. p-Value* and p-value† compared to control and unlikely groups using the Mann-Whitney U test, respectively. The definite group exhibited characteristic clinical and imaging features of HDLI and were admitted to intensive care unit admission for acute respiratory distress syndrome. The probable group partially met the clinical, imaging, or pathological criteria for HDLI but did not fulfill all diagnostic requirements. The unlikely group had documented exposure to humidifier disinfectants but lacked clinical, imaging, or pathological evidence consistent with HDLI. The diagnostic criteria for HDLI are presented in Table S1. —, no data; HDLI, humidifier disinfectant–associated lung injury; ND, not done; NA, not available; HD, humidifier disinfectant; SD, standard deviation.

analyze plasma samples from diagnosed patients. Our objective was to uncover potential targets for biomarker development and gain deeper insights into the pathogenesis of HDLI.

Methods

Study Population

The study comprised 60 children and 107 adults with lung injuries caused by exposure to specific humidifier disinfectants containing PHMG (Table 1 and Table 2). All the HDLI patients were recruited from the physical health monitoring program at the Humidifier Disinfectant Health Center, an established cohort at the Asan Medical Center, between 2014 and 2016. Diagnostic criteria for HDLI were established based on the patients' clinical, pathological, and radiological characteristics.[20] This approach was designed not only to determine whether the lung disease resulted solely from humidifier disinfectant exposure but also to assess the severity of the condition. HDLI patients were classified into three groups: definite, probable, or unlikely. The "definite" group exhibited typical clinical and imaging characteristics of HDLI, with most patients having a history of admission to the intensive care unit for acute respiratory distress syndrome. The "probable" group included individuals whose clinical, imaging, or pathological findings partially aligned with HDLI, though they did not meet all criteria. Despite confirmed exposure to humidifier disinfectants, a definitive diagnosis could not be established, and the possibility of other diseases could not be entirely excluded. The "unlikely" group had been exposed to humidifier disinfectant but lacked confirmed clinical, imaging, and/or pathological characteristics of HDLI, suggesting a heterogeneous clinical spectrum or very mild HDLI without definitive clinical and radiological features at that time. Further details about the criteria and classification[20] of HDLI are shown in Table S1.

In addition, 20 children with asthma (5–10 y of age) and 7 children with bronchiolitis obliterans (BO), a chronic respiratory disease (3–18 y of age), were recruited in 2018 from the Childhood Asthma and Atopy Center at Asan Medical Center (Table S2). Asthma was diagnosed in patients who had at least one wheezing episode in the past year. BO was diagnosed in patients with a history of early childhood respiratory infection, persistent respiratory symptoms, and obstructive patterns on chest computed tomography (CT), such as mosaic attenuation, air trapping, or bronchial abnormalities. Diagnoses were confirmed by two independent pediatric pulmonologists.[21]

The control group comprised 20 healthy children from the 2015 Panel Study of Korean Children, representing the general population cohort,[22] and 25 healthy parents from the Childhood Origin of Asthma and Allergic Diseases cohort (2008–2017),[23] all without a history of chronic respiratory disease. Their nonuse of humidifier disinfectants was confirmed through a questionnaire. The control participants were randomly selected, but their age ranges matched those of the disease group. All study participants were South Korean, and children were defined as individuals under the age of 18 y.

Plasma samples were collected at cohort enrollment, centrifuged at $3,000 \times g$ for 10 min, and stored at $-70^\circ C$ without prior thawing until metabolomic analysis. Serum was collected in 2.0 mL EDTA tubes (BD Vacutainer). These samples were part of the cohort study and were not collected specifically for this

Table 2. Study population of adults by HDLI groups in the physical health monitoring program (Asan Medical Center, South Korea, 2014–2016, $n = 132$).

	Control ($n = 25$)	Unlikely ($n = 55$)		Probable ($n = 20$)			Definite ($n = 32$)		
Adults	Mean ± SD	Mean ± SD	p^*	Mean ± SD	p^*	$p^\dagger$	Mean ± SD	p^*	$p^\dagger$
Age (y)	32.92 ± 3.44	44.87 ± 13.34	<0.001	44.70 ± 12.31	<0.001	0.981	41.03 ± 7.76	<0.001	0.275
Sex (n)									
Male	13	25	—	11	—	—	7	—	—
Female	12	30	—	9	—	—	25	—	—
Airborne HD concentration ($\mu g/m^3$)	NA	183.40 ± 183.31	—	136.81 ± 102.01	—	0.302	188.84 ± 337.41	—	0.191
Total duration of HD use (h)	NA	9,936.87 ± 10,882.07	—	9,620.21 ± 8,206.02	—	0.407	10,987.03 ± 8,079.32	—	0.09

Note: Data are presented as the mean ± SD. p-Value* and p-value† represent comparisons with the control and unlikely groups, respectively, using the Mann-Whitney U test. The definite group had distinct clinical and imaging characteristics of HDLI and required admission to the intensive care unit for acute respiratory distress syndrome. The probable group exhibited some clinical, imaging, or pathological features of HDLI but did not fully meet the diagnostic criteria. The unlikely group had confirmed humidifier disinfectant exposure but lacked clinical, imaging, or pathological findings indicative of HDLI. The diagnostic criteria for HDLI are provided in Table S1. HDLI, humidifier disinfectant–associated lung injury; NA, not available; HD, humidifier disinfectant; SD, standard deviation.

study. The maximum storage duration before analysis was 10 y. The study protocols were approved by the institutional review board of Asan Medical Center (2018–0663) for metabolomic analysis. Human-derived samples were obtained from studies approved under additional IRBs, including the Physical Health Monitoring Program at the Humidifier Disinfectant Health Center (2015–0510), the Panel Study of Korean Children (2015–0907), the Cohort for Childhood Origin of Asthma and Allergic Diseases (2008–0616), and the Childhood Atopy and Allergy Center (2015–1031). Written informed consent was obtained from each participant or parent following a detailed explanation of the study.

Estimation of Humidifier Disinfection Exposure

Exposure assessment was conducted through questionnaires administered by an environmental health specialist. To improve the accuracy of exposure assessment, the Korean government obtained photographs of used humidifier disinfectant products and purchase receipts from the participants. The airborne disinfected concentration was calculated as[24] disinfectant concentration dissolved in the product times average daily humidifier disinfectant usage (μg)/volume of the room (m^3). The disinfectant concentration of each product was determined based on an investigation conducted by the Korea Center for Disease Control and Prevention (KCDC).[25] The questionnaire collected data on the amount and duration of disinfectant use, the size of the rooms where humidifiers were used, and other relevant factors (see Supplemental Material, "Questionnaire").

Plasma Metabolite Profiling Using Ultra-High Performance Liquid Chromatography with Quadrupole Time-of-Flight Mass Spectrometry

Plasma samples were collected at cohort enrollment and immediately stored at −70°C. For mass spectrometry analysis, they were processed in two batches (Figure 1). All samples within each batch were thawed simultaneously, with one batch designated for the child cohort and the other for the adult cohort. The child samples, categorized into control, definite, probable, unlikely, BO, and asthma groups, were processed simultaneously. Adult samples, divided into control, definite, probable, and unlikely groups, were processed on the same day. To minimize potential bias, the analysis order was randomized across all groups. Prepared

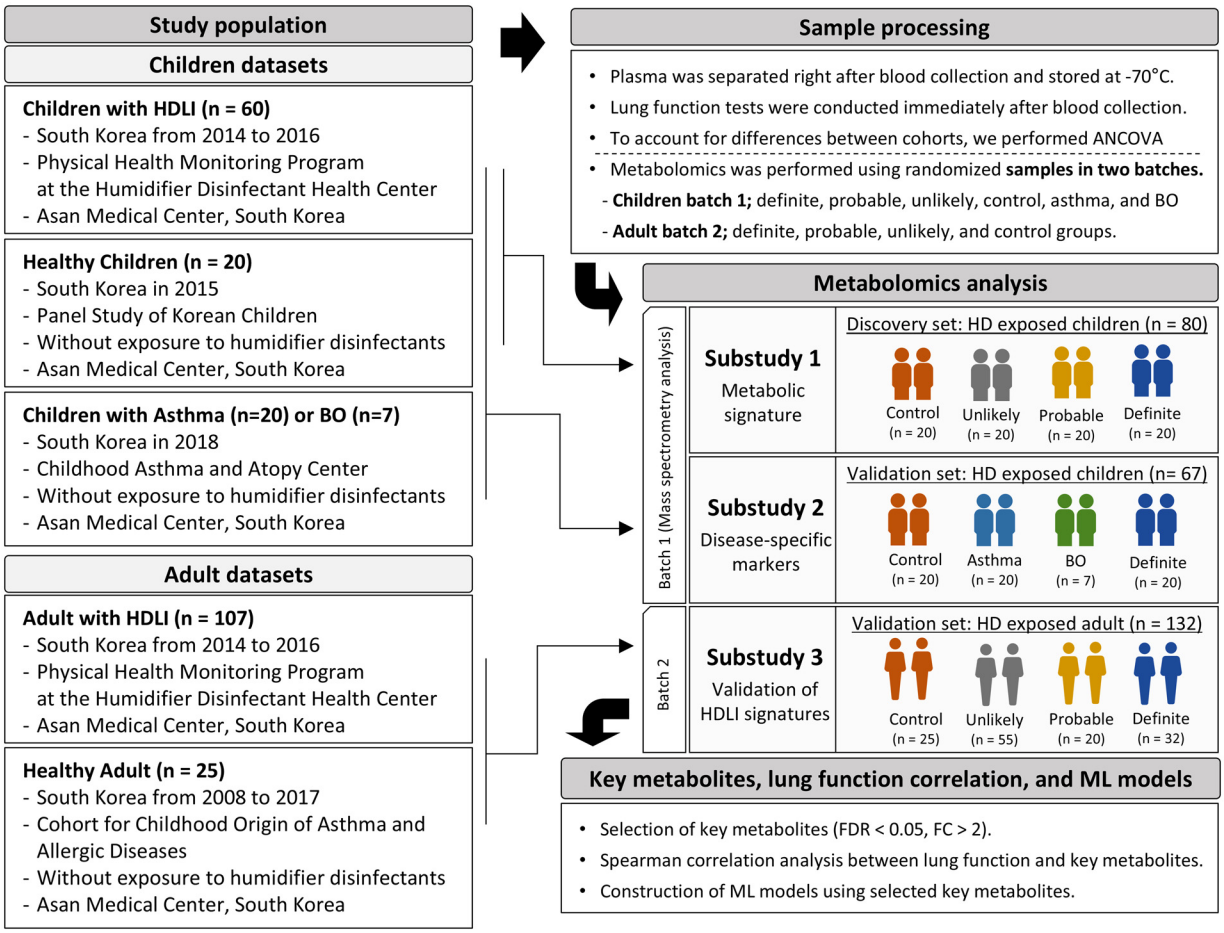

Figure 1. Study population and metabolomic analysis process. Samples from multiple cohorts were analyzed and processed at Asan Medical Center, Seoul, South Korea. Upon collection, the samples underwent the same preprocessing method and were immediately frozen at −70°C. All samples were randomized before selection and analyzed in two batches: one for children and one for adults, to minimize batch effects. The diagnostic criteria for HDLI are shown in Table S1. The definite group had typical clinical and imaging features of HDLI, and all were admitted to the intensive care unit for acute respiratory distress syndrome. The probable group showed partial clinical, imaging, or pathological alignment with HDLI criteria but did not meet all criteria. The unlikely group had confirmed humidifier disinfectant exposure but lacked clinical, imaging, or pathological findings consistent with HDLI. Asthma patients who had at least one wheezing episode in the past year were diagnosed by a physician. BO was diagnosed based on a history of early childhood respiratory infection, persistent symptoms, lack of response to inhaled corticosteroids or bronchodilators, and obstructive patterns observed on a chest CT, including mosaic attenuation, air trapping, or bronchial abnormalities. Note: ANCOVA, analysis of covariance; BO, bronchiolitis obliterans; CT, computed tomography; FDR, false discovery rate; FC, fold change; HDLI, humidifier disinfectant–associated lung injury.

plasma was mixed with 80% methanol at a 1:6 ratio and incubated at 4°C for 60 min. After centrifugation at 12,000 × *g* for 15 min, the supernatants were injected into the ultra-high performance liquid chromatography with quadrupole time-of-flight mass spectrometry (UPLC-q/TOF MS) system. The chromatographic system comprised a Waters Acquity UPLC (Waters) coupled with a Synapt G2-Si quadrupole time-of-flight mass spectrometer (Waters). Chromatographic separation was achieved using an Acquity UPLC BEH C18 column (2.1 mm × 100 mm, 1.7 μm). The mobile phases, delivered at a rate of 0.4 mL/min, were 0.1% formic acid (v/v) in water (phase A) and 0.1% formic acid (v/v) in acetonitrile (phase B). Mass spectra (MS) were acquired in both positive and negative modes within the *m/z* range of 50–1,000. Each biological sample was analyzed once, and the sample arrangement was randomized to avoid technical bias. Quality control (QC) samples were prepared by pooling equal aliquots from all analytical samples and were introduced into the chromatographic system every seven samples throughout the analytical run.

Data Processing

The raw MS data were preprocessed using Progenesis QI software (Nonlinear Dynamics), which included automatic alignment for retention time (RT), peak picking, deconvolution, and peak quality assessment. Following preprocessing, the peak intensity of each sample was adjusted by subtracting the mean blank intensity for each feature. Features with more than 50% missing values in every group were excluded from further analysis.

Metabolite Identification

Metabolite annotation was performed by analyzing tandem mass (MS^2) fragmentation patterns using CFM-ID 3.0.[26] We conducted a reevaluation by manually comparing experimentally acquired MS^2 spectra with those of potentially annotated compounds from the Human Metabolome Database (HMDB; version 5.0) to ensure accurate metabolite annotation.[27] Annotation confidence levels were classified per the guidelines of the Metabolomics Standard Initiative (MSI).[28] The classification includes four levels of confidence in metabolite identification. Level 1 represents compounds confidently identified through comparison with reference standards; Level 2 involves the putative annotation of compounds based on spectral similarity to known compounds in public or commercial spectral libraries; Level 3 encompasses the putative annotation of compound classes based on spectral similarity to a chemical class; and Level 4 pertains to unidentified compounds. Oxidized lipids exhibit structural diversity, existing in various forms such as epoxides, hydroxides, hydroperoxides, aldehydes, or carboxylic acids. However, this diversity complicates the precise determination of oxidized lipid structures via liquid chromatography–tandem mass spectrometry (LC-MS/MS). Consequently, we characterized the oxidized lipids by specifying the number of carbons, double bonds, and oxygen atoms, providing an overview of their molecular composition without detailed annotation (Table S3).

Pulmonary Function Test

Pulmonary function was assessed using three parameters: forced vital capacity (FVC), which measures total exhaled air volume after a deep breath; forced expiratory volume in one second (FEV1), which indicates the volume exhaled during the first second of the FVC test; and hemoglobin-corrected diffusing capacity of the lungs for carbon monoxide (cDLCO), which evaluates oxygen transfer efficiency. These clinical parameters were measured using a Vmax229D (SensorMedics) following the recommendations of the American Thoracic Society (ATS)/European Respiratory Society (ERS).[29] Pulmonary function was measured at enrollment, on the same day as the blood sample collection. FVC and FEV1 were assessed in all groups, including control, asthma, HDLI diagnosis, and BO, whereas cDLCO was measured only in HDLI and BO patients.

Machine Learning

We trained and validated six machine learning (ML) models—logistic regression, support vector machines (SVM), random forest, decision tree, K-nearest neighbor (KNN), and naïve Bayes—to evaluate the diagnostic potential of metabolic signatures for HDLI. Key features (putative metabolites) were identified through a univariate comparison between the definite and control groups. Features were selected based on a false discovery rate (FDR)-adjusted *p*-value of <0.05 and a fold change of >2.0. Among the metabolites showing significant differences, we focused on those with relative standard deviation (RSD) values in QC samples below 30%. We used a metabolomics dataset comprising 107 children, selecting 47 features (intensity of differential metabolites) and labeling the dataset with binary values: 1 for the HDLI group (definite, probable, and unlikely; $n = 60$) and 0 for groups without HDLI ($n = 47$). The dataset, including both the HDLI group and the non-HDLI group, was stratified and split into training ($n = 74$) and testing sets ($n = 33$) in a 7:3 ratio for model development and evaluation, employing a stratified random sampling method for the division. Before training the ML algorithms, the training dataset was scaled to zero mean and unit standard deviation using the standard scaler function. We evaluated the performance of all trained classifiers using a test dataset comprising 33 test samples. The parameters used in these models are listed in Table S4.

Statistical Analysis

Statistical analysis was performed using Python (version 3.9.12) along with the NumPy (version 1.21.5), Pandas (version 1.4.2), Scipy (version 1.7.3), statsmodels (version 0.13.2), and sklearn (version 1.0.2) libraries. Data normality was assessed using the Shapiro-Wilk test. If the data were not normally distributed, the Mann-Whitney *U*-test was used. If the data were normally distributed, statistical comparisons between groups were conducted using either Student's *t*-test or Welch's *t*-test, depending on the homogeneity of variances assessed by Levene's test. *p*-Values were adjusted using the Benjamini-Hochberg procedure to control the FDR. For comparisons involving more than two groups, statistical significance was determined using one-way analysis of variance (ANOVA) followed by the Bonferroni post hoc test for multiple comparisons. An analysis of covariance (ANCOVA) was performed to account for the effects of confounders on the variables that show differences between groups. Multivariate analyses, including principal component analysis (PCA) and partial least squares discriminant analysis (PLS-DA), were conducted, with features scaled with Pareto scaling. The PLS-DA models were built separately for the positive and negative modes, using all detected metabolites for each mode (1,254 mass ions in the positive mode and 730 mass ions in the negative mode). Model evaluation involved 5-fold cross-validation, with PLS-DA quality assessed by R^2Y (fit) and Q^2 (prediction). To prevent overfitting, a 100-iteration permutation test was conducted, with *p*-values calculated using MetaboAnalyst 5.0.

Data Availability

The metabolomic datasets and the code used for the analyses are available on GitHub (https://github.com/jinwoo3239/HDLI).

Results

Study Population and Selection Process

We designed this study to identify the metabolic signature of individuals with HDLI. Participants diagnosed with HDLI were selected from the Physical Health Monitoring Program, which included 750 individuals. Among the pediatric patients, 20 were classified as definite, and to maintain consistency, 20 probable and 20 unlikely cases were randomly selected. Other pediatric patients with respiratory diseases, including asthma and BO, were recruited from the Childhood Atopy and Allergy Center. During the recruitment period, 20 pediatric patients with asthma were enrolled, whereas only 7 BO cases were available due to its low prevalence. The control group was selected from the cohort of Panel Study of Korean Children,[22] a longitudinal study investigating child development and allergic diseases. A total of 2,150 mother–child pairs were recruited, of whom 1,573 completed questionnaires on allergic diseases. Another 42 pairs were excluded due to missing exposure or demographic data, resulting in a final sample of 1,531 pairs. From these eligible individuals, age- and sex-matched pediatric controls were randomly selected based on predefined criteria, including South Korean nationality, absence of chronic respiratory or allergic conditions, and no history of humidifier disinfectant exposure. All study participants were anonymized, and random sampling was applied. The study population and analysis process are summarized in Figure 1.

Untargeted Metabolite Profiling in Children with HDLI

We initially examined plasma metabolites in children with HDLI, categorizing the subjects into four groups ($n = 20$ per group): definite, probable, unlikely, and control. A total of 1,254 mass ions were detected in positive mode, and 730 in negative mode, at specific RT points. To identify the distinctive metabolic signatures associated with HDLI, we compared the most severely affected group (definite) with the control group. For exploratory data analysis, we employed PCA and PLS-DA to assess the metabolic distribution between the two groups (Figure 2A; Figure S1). Both PCA and PLS-DA showed a clear separation between the two groups, suggesting that HDLI was associated with distinct plasma metabolite profiles. Although the 2D plot did not distinctly separate the four groups, the PLS-DA model nevertheless exhibited robust classification ability (Figure 2A). An $R^2 > 0.68$ indicated that the model accounted for more than 68% of the variance, and a $Q^2 > 0.51$ confirmed its predictive accuracy. Finally, a permutation test p-value of <0.05 established the model's statistical significance (Figure S2).

Identification of Key Metabolic Signatures Linked to HDLI

To identify key molecules associated with HDLI, a univariate comparison was conducted between the definite and control groups. Features (putative metabolites) were selected based on an FDR-adjusted p-value of <0.05 and a fold change of >2.0 (Table S3). Using these criteria, we identified 47 metabolites, which were designated as key metabolites for further analysis. After annotation in the Human Metabolome Database,[27] 61.7% of the selected key metabolites were classified as oxidized lipids, including 14 oxidized fatty acids (oxFA) and 15 oxidized phosphatidylcholines (oxPC) (Figure 2B; Table S3). Given that key metabolites were statistically identified by comparing the definite and control groups, we further analyzed their peak intensities across all four groups (Figure 3; Excel Table S1). We specifically focused on oxidized lipids, noting that their intensities varied by group. The intensity of hydroxylpalmitic acid was 1.44 times higher in the unlikely group, 1.72 times higher in the probable

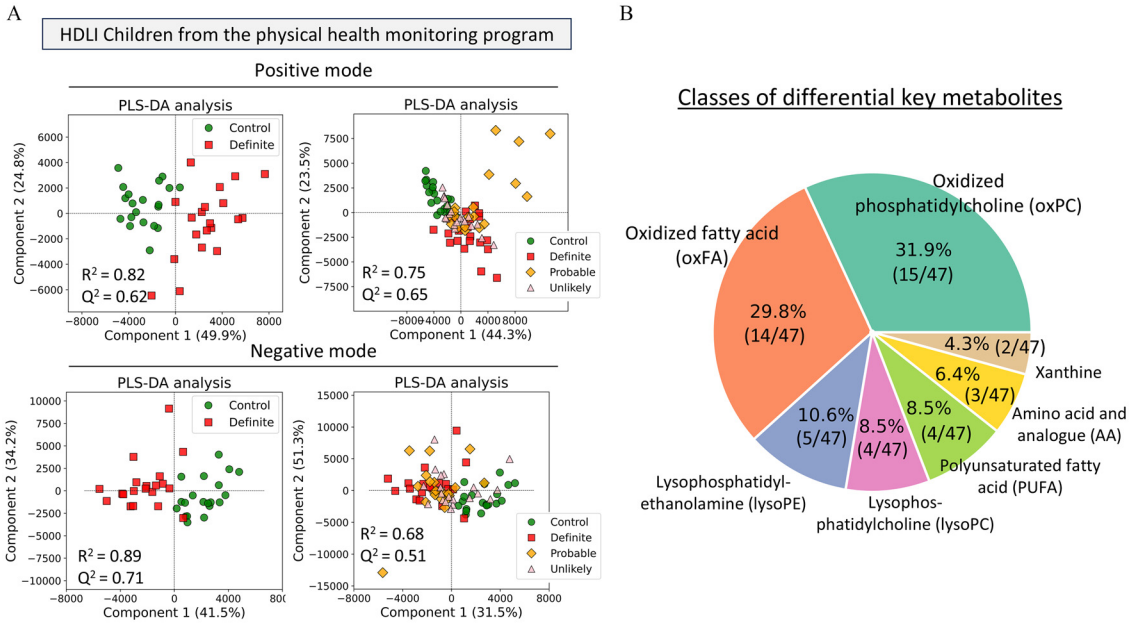

Figure 2. Multivariate statistical analysis of otherwise healthy children with HDLI recruited from South Korea through the Physical Health Monitoring Program at the Humidifier Disinfectant Health Center at the Asan Medical Center between 2014 and 2016 ($n = 80$). (A) PLS-DA models were constructed separately for the positive and negative modes of ESI mass spectrometry, incorporating all detected metabolites in each mode (1,254 mass ions in the positive mode and 730 mass ions in the negative mode. Features were scaled using Pareto scaling prior to multivariate analysis. Model parameters were determined through 5-fold cross-validation, with performance assessed evaluated using the coefficient of determination (R^2) and the cross-validated coefficient of determination (Q^2). (B) Key metabolites with significant differences in plasma levels between the definite and control groups were classified into chemical categories. The numbers indicate the count of metabolites in each class relative to the total number of key metabolites. Note: ESI, electrospray ionization; HDLI, humidifier disinfectant–associated lung injury; PLS-DA, partial least squares discriminant analysis.

group, and 2.34 times higher in the definite group in comparison with the control group.

Metabolic Signatures of HDLI Compared with Asthma and BO

To determine whether the key metabolites identified in children with HDLI were associated with humidifier disinfectant exposure, we compared metabolite profiles from participants with other respiratory diseases, including asthma and BO. The groups comprised HDLI definite ($n = 20$), healthy control ($n = 20$), asthma ($n = 20$), and BO ($n = 7$), with the asthma and BO groups having no history of humidifier disinfectant exposure. Multivariate analysis revealed that the HDLI definite group was distinctly separate from both the asthma and BO groups, indicating significant metabolic differences in HDLI (Figure S3). We further compared the level of the 47 key metabolites associated with HDLI against those in the asthma and BO groups and observed that oxFA and oxPC levels were significantly higher in the HDLI groups than in the asthma and BO groups (Figure 4; Excel Table S2). However, key metabolites, including linolenic acid, eicosapentaenoic acid, and arachidonic acid, also exhibited significant differences from control in the asthma and BO groups. Our study showed that arachidonic acid levels were elevated in both the asthma and HDLI groups in comparison with controls. Despite these similarities, a statistically significant difference was observed between the asthma and HDLI groups, with the HDLI group exhibiting higher arachidonic acid levels (Figure S4; Excel Table S3). Specifically, arachidonic acid levels in the asthma group were 5.83 times higher than in the controls, whereas in the definite group, the levels were 8.33 times higher. Furthermore, because of the significant age differences between the groups (Table S2), we applied ANCOVA to adjust for age. However, even after this adjustment, the metabolic differences between the groups remained statistically significant (Excel Table S4).

Validation of HDLI-Associated Key Metabolites in the Adult Cohort

We validated the differential metabolites discovered from children's samples in an independent cohort of adult HDLI patients ($n = 132$). An untargeted metabolomics analysis was performed on adult samples, classified into the same four groups as in the children's HDLI classification: definite ($n = 32$), probable ($n = 20$), unlikely ($n = 55$), and control ($n = 25$). All key metabolites showed statistically significant differences, with FDR-adjusted p-values of <0.05, confirming that the metabolites identified in children could significantly differentiate between the control and definite groups in adults (Figure 5; Table S5 and Excel Table S5).

Relationship between Key Metabolites and Parameters of Lung Function

We examined the relationship between key HDLI metabolites and lung function parameters in children (Figure 6A; Excel Table S6). After conducting lung function assessments [comprising FVC (%), FEV1 (%), and cDLCO (%)], we observed a negative correlation between lung function parameters and lipid-related molecules. Specifically, nine metabolites [lysoPC (P-16:0), lysoPC (P-18:0), HOTE, DiHODE, DiHETrE, oxPC36:5 + 1O, oxPC38:7 + 2O, oxPC38:6 + 2O] exhibited significant negative correlations with all lung function parameters. Among these, oxPC38:6 + 2O demonstrated a statistically significant association with FVC [Spearman's rho (ρ) = −0.27], FEV1 ($\rho = -0.28$), and cDLCO ($\rho = -0.36$) (Figure 6B). In addition, DiHETrE [6.41_337.2367; retention time (minute)_m/z valueand oxPC38:6 + 2O (9.62_838.5595) showed moderately negative correlations with cDLCO ($\rho = -0.38$ and −0.36, respectively, Figure 6B). Conversely, uric acid (0.66_167.0206) was positively correlated with cDLCO ($\rho = 0.41$).

ML for Classifying HDLI Using Metabolic Signatures

We conducted a receiver operating characteristic (ROC) curve analysis and computed the area under the curve (AUC) to compare the diagnostic accuracies of the classifiers (Figure 7A). All models were trained on the 47 selected key metabolites and achieved AUC values >0.95, which indicates a strong ability to differentiate between the two classes. We also evaluated the performance of the ML models using various evaluation metrics, including accuracy, precision, recall, and F1 score (Figure 7B; Table S6). In medical diagnostics, recall and precision are essential because they reflect the rates of false positives (incorrectly diagnosing disease) and false negatives (missing actual cases). All trained models exhibited precision values of 0.84–0.95 and recall values of 0.94–1.0, highlighting their effectiveness in correctly identifying positive cases. Among the models, the random forest model exhibited the highest diagnostic performance, achieving an impressive accuracy of 0.97, a precision score of 0.95, an F1 score of 0.97, and a perfect recall of 1.00.

Discussion

In this study, we conducted a metabolomics analysis to investigate the underlying pathogenesis and metabolic signatures of HDLI. We identified 47 key plasma metabolites that exhibited significantly different levels between the control and definite groups in children. Among these metabolites, 29 (61.7%) were oxidized lipids (oxFA and oxPC), suggesting that oxidative stress plays a role in HDLI (Figure 2). These differences in key metabolites were validated in an independent cohort of adult HDLI patients (Figure 5). Furthermore, when compared with asthma and BO patients who had never been exposed to humidifier disinfectants, these key metabolites were identified as specific signatures of HDLI (Figure 4), indicating a potential association between HDLI and these key metabolites. In addition, key metabolites showed a negative correlation with lung function in the children's participants (Figure 6). We also evaluated the diagnostic performance of these key metabolites for classifying HDLI, achieving an accuracy of 0.97, a precision score of 0.95, an F1 score of 0.97, and a recall of 1.00 (Figure 7). These results reinforced the hypothesis that increased ROS, triggered by humidifier disinfectant, can be detrimental to human health.

The study subjects who developed HDLI had been exposed to humidifier disinfectants containing PHMG. Because of its strong antimicrobial properties,[30] PHMG is added to humidifiers to control microbes' growth. Its cationic guanidine group[31] enables it to electrostatically interact with and bind to cellular membranes,[32] resulting in the leakage of cytoplasmic components and the activation of membrane-bound enzymes, leading to significant membrane disruption. A previous *in vitro* study demonstrated that PHMG can migrate to the cellular membranes of lung epithelial cells.[33] Subsequently, it may translocate to the endoplasmic reticulum (ER) and mitochondria via endocytosis or direct penetration. Internalized PHMG-p can disrupt ER function and activate the PERK signal-transduction pathway of the unfolded protein response (UPR).[33] Under prolonged and excessive stress, PHMG may ultimately activate the mitochondria-associated apoptotic pathway,[33] resulting in ROS generation caused by mitochondrial dysfunction.[33,34]

Elevated levels of oxidized lipids in HDLI patients in comparison with healthy controls suggest a correlation between HDLI

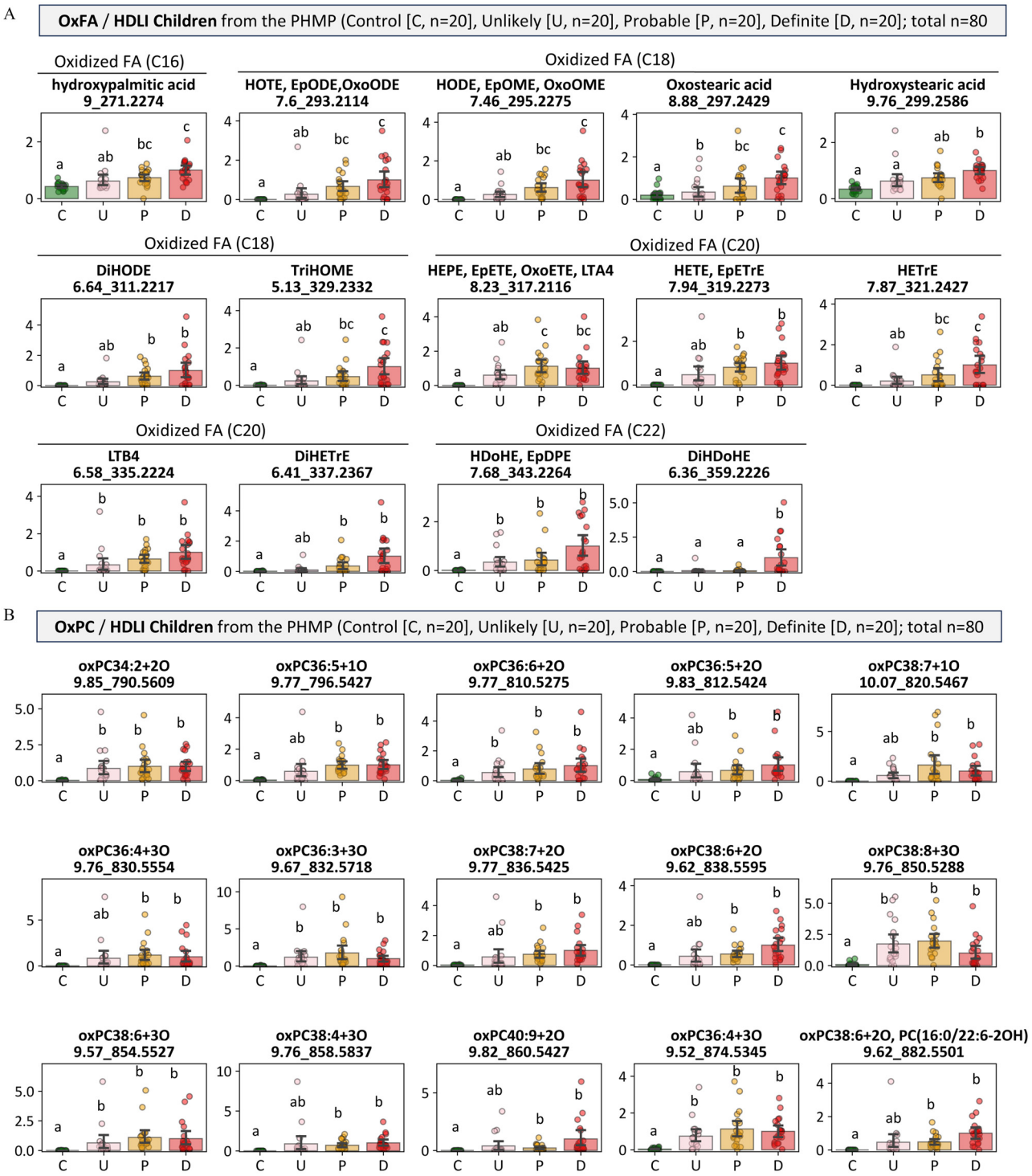

Figure 3. Metabolic signature of oxidized lipids in the plasma of South Korean children diagnosed with HDLI, enrolled in the Physical Health Monitoring Program at the Humidifier Disinfectant Health Center at Asan Medical Center between 2014 and 2016 ($n = 80$). We compared the peak intensities of the key metabolites, oxFA (A) and oxPC (B), across four groups based on clinical HDLI criteria. oxPCs are represented by the total number of carbon atoms, the number of double bonds, and the additional oxygen atoms in the molecule. For comparisons involving more than two groups, statistical significance was determined using a one-way ANOVA followed by the Bonferroni post hoc test for multiple comparisons. The results of pairwise comparisons are displayed using the compact letter display ($p < 0.05$). The *y*-axis represents relative peak intensity. The black vertical lines indicate 95% CIs. The corresponding numerical data is presented in Excel Table S1. Note: ANOVA, analysis of variance; CI, confidence interval; HDLI, humidifier disinfectant–associated lung injury; oxFA, oxidized fatty acid; oxPC, oxidized phosphatidylcholine; PHMP, Physical Health Monitoring Program.

and lipid peroxidation (Figure 2B). Lipid peroxidation is a well-documented biochemical process in which ROS and free radicals react with unsaturated fatty acids (FAs) in cell membranes, leading to the formation of oxFAs and other oxidized lipids.[35] These findings align with previous *in vitro* studies demonstrating that PHMG can generate ROS,[33] thereby supporting the association between HDLI and oxidative stress. The key metabolites identified in this study provide insights into HDLI pathogenesis,

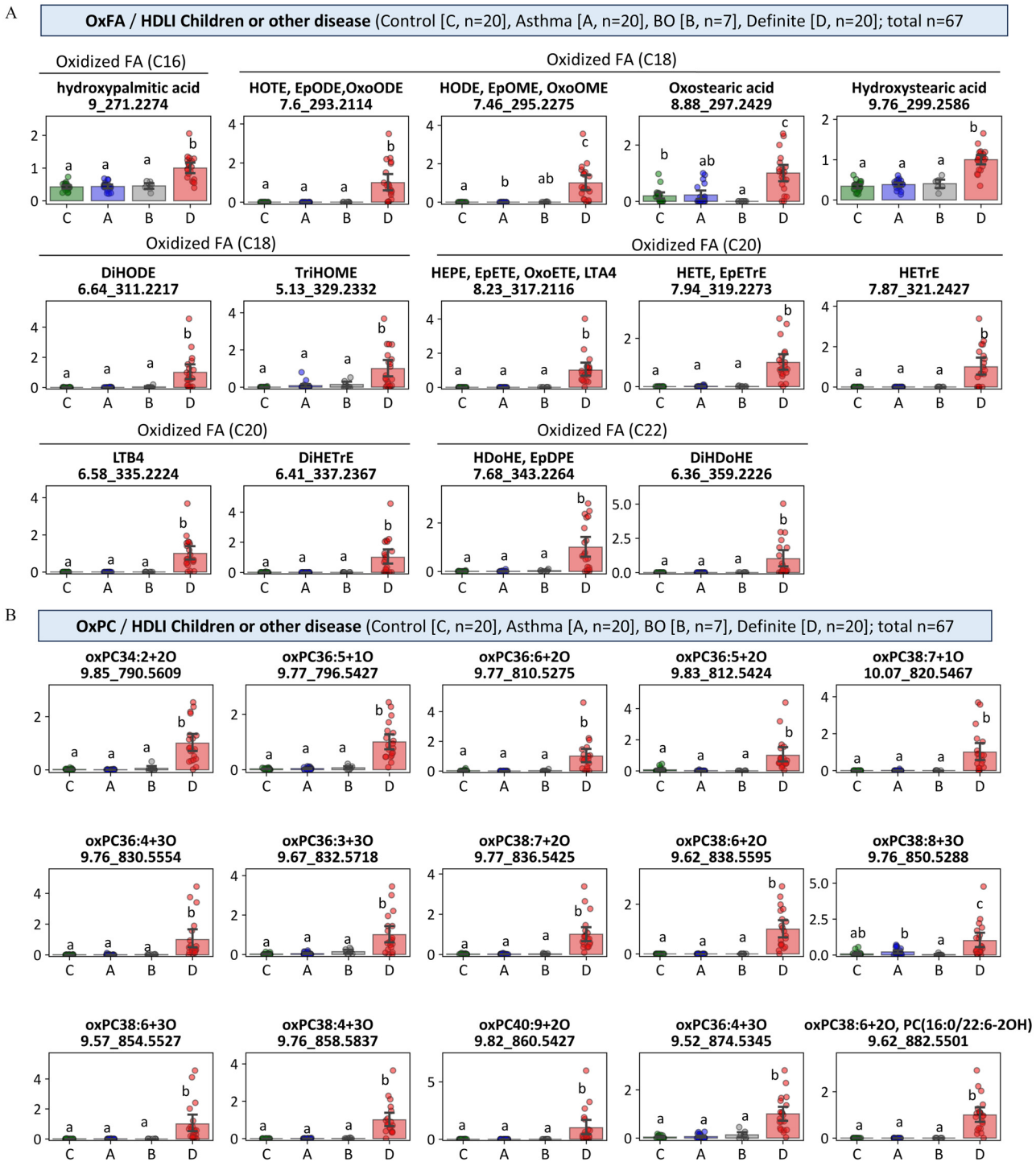

Figure 4. HDLI-specific metabolic signatures compared with asthma and bronchiolitis obliterans in children recruited from the Childhood Asthma and Atopy Center and the Humidifier Disinfectant Health Center at Asan Medical Center ($n = 67$, 2014–2016 for HDLI; 2018 for asthma and BO). The intensities of key metabolites oxFA (A) and oxPC (B) were compared between children with HDLI and those with asthma or BO. oxPCs are characterized by the total number of carbon atoms, double bonds, and additional oxygen atoms. One-way ANOVA was used for group comparisons, while statistical comparisons between two groups were conducted using either Student's *t*-test or Welch's *t*-test, depending on the homogeneity of variances, as assessed by Levene's test. *p*-Values were adjusted using the Bonferroni procedure to control the FDR. The results of adjusted pairwise comparisons are summarized with a compact letter display ($p < 0.05$). The *y*-axis represents the relative peak intensity. The black vertical lines indicate 95% CIs. The corresponding numerical data are presented in Excel Table S2. Note: ANOVA, analysis of variance; BO, bronchiolitis obliterans; CI, confidence interval; FDR, false discovery rate; HDLI, humidifier disinfectant–associated lung injury; oxFA, oxidized fatty acid; oxPC, oxidized phosphatidylcholine.

underscoring the role of oxidative stress. Through a comprehensive approach, including robust statistical analysis and cross-cohort assessments (Figure 1), our study provides compelling evidence of the association between HDLI and ROS, reinforcing the significance of these metabolic signatures in understanding the HDLI disease.

Based on our findings, we propose a pathogenesis model of HDLI in humans (Figure S5). PHMG localizes to the ER, leading

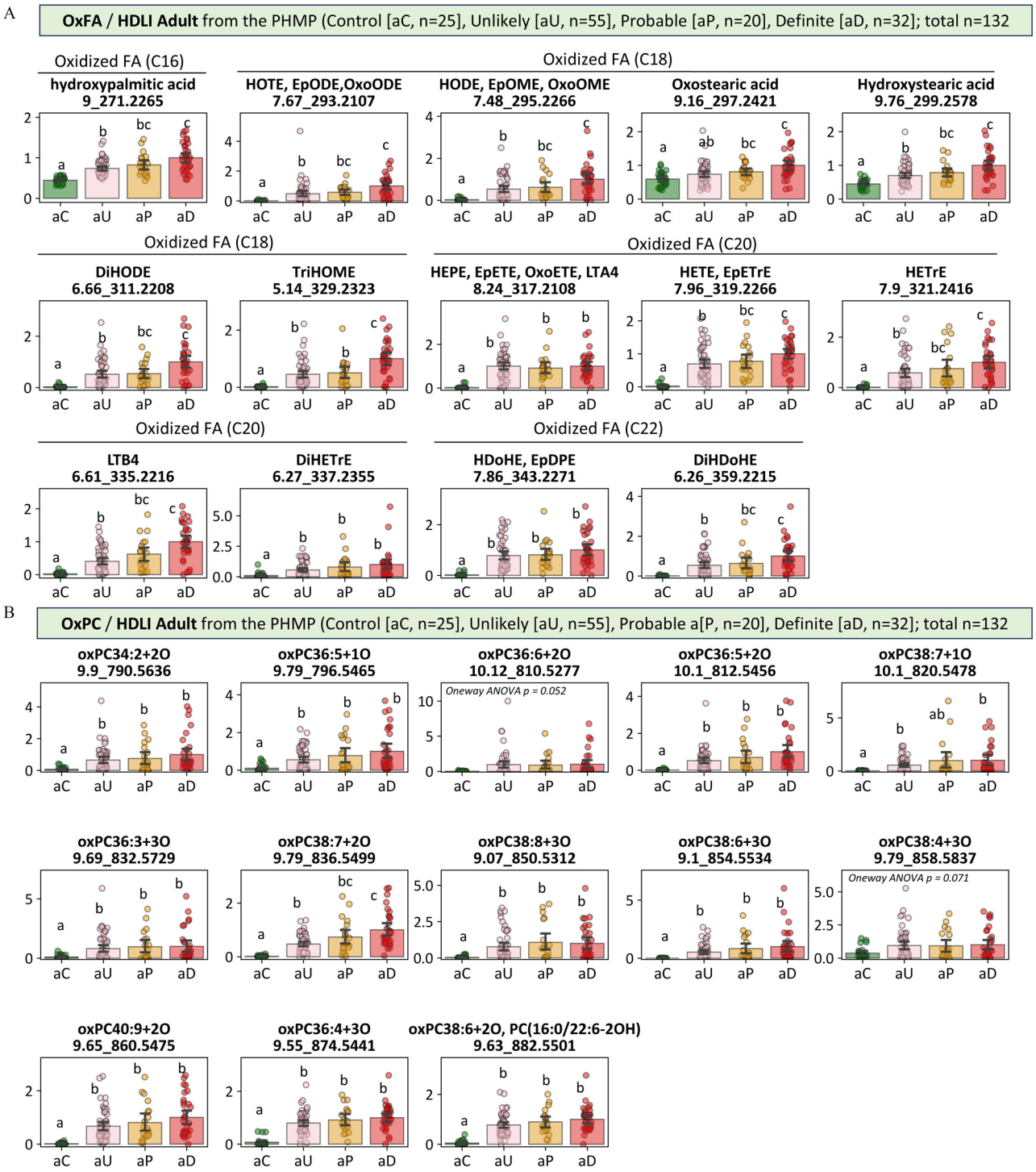

Figure 5. Validation of key metabolites discovered in children using adult samples from the Physical Health Monitoring Program at the Humidifier Disinfectant Health Center in South Korea between 2014 and 2016 ($n = 132$). We compared the peak intensities of key metabolites, oxFA (A) and oxPC (B), across four adult groups classified according to clinical HDLI criteria. oxPCs are characterized by the total number of carbon atoms, the number of double bonds, and the total count of oxygen atoms in the molecule. For comparisons involving more than two groups, statistical significance was determined using a one-way ANOVA followed by the Bonferroni post hoc test for multiple comparisons. The results of these comparisons are displayed using a compact letter display ($p < 0.05$). The *y*-axis represents relative peak intensity. The black vertical lines indicate 95% CIs. The corresponding numerical data are presented in Excel Table S5. Note: ANOVA, analysis of variance; HDLI, humidifier disinfectant–associated lung injury; PHMP, Physical Health Monitoring Program; oxFA, oxidized fatty acid; oxPC, oxidized phosphatidylcholine.

to ER stress and mitochondrial apoptosis as initial triggers in ROS generation. The induced ROS molecules then target the cellular membrane, affecting polyunsaturated fatty acids (PUFA), in a process known as lipid peroxidation. Consequently, oxidized lipid levels can increase in plasma, disrupting cellular membrane integrity and function. Lipid peroxidation may also contribute to inflammation, which can activate enzymes[36,37] such as cyclooxygenase (COX) and lipoxygenase (LOX). These enzymes convert arachidonic acid into proinflammatory eicosanoids, ultimately inducing inflammation.[38]

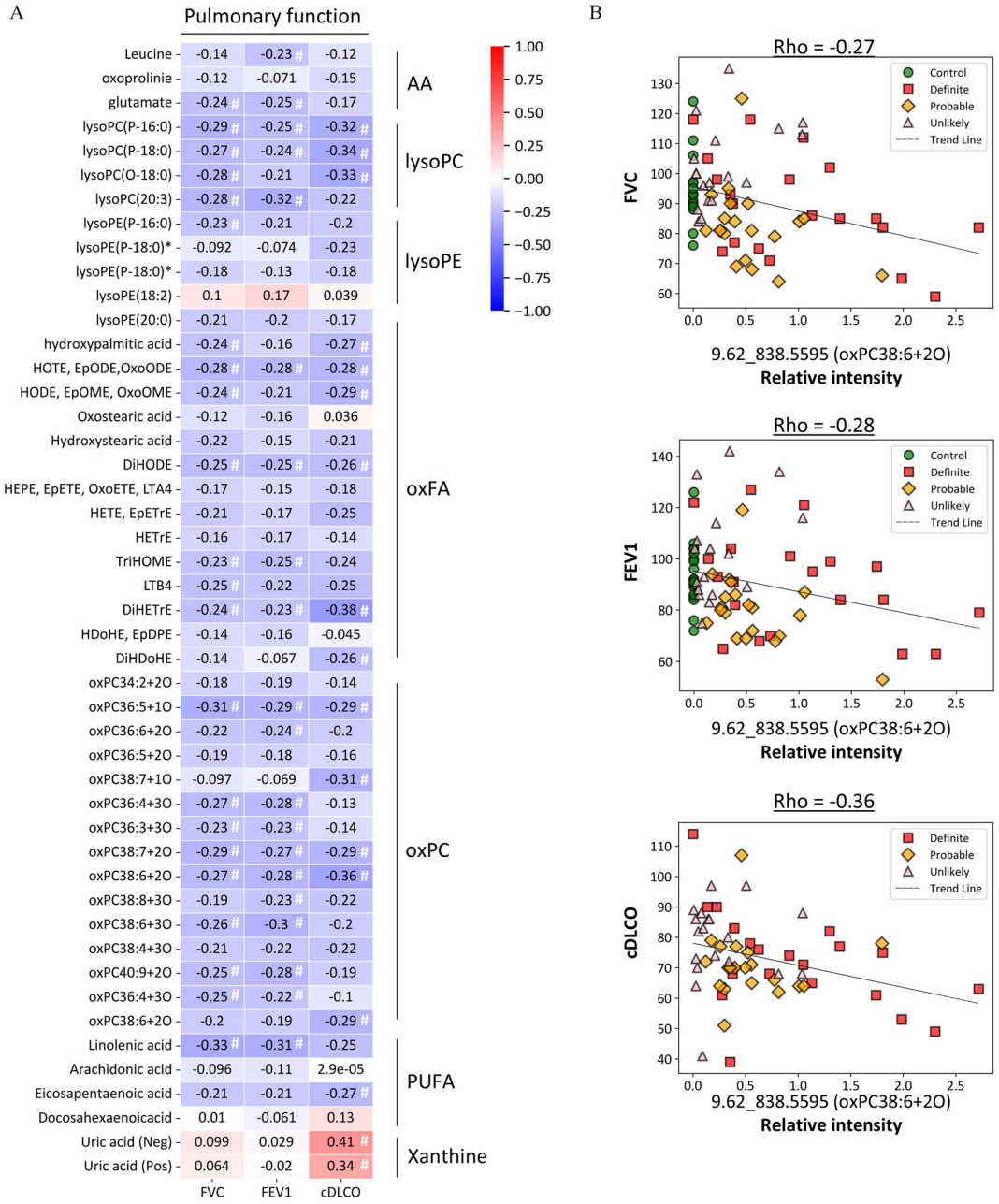

Figure 6. Spearman's correlation analysis between key metabolites and lung function parameters in children diagnosed with HDLI, recruited from the Physical Health Monitoring Program at the Humidifier Disinfectant Health Center at Asan Medical Center from 2014 to 2016 ($n = 80$). (A) The correlation coefficients (Spearman's ρ) are displayed in a heat map. Red indicates a positive correlation between variables, and blue indicates a negative correlation. The hash symbol (#) indicates statistical significance ($p < 0.05$). Correlation analysis for cDLCO was conducted within the HDLI groups (definite, probable, and unlikely; $n = 60$), whereas the correlation analysis for other clinical parameters encompassed all four groups ($n = 80$). The analyzed p-values are presented in Excel Table S6. (B) Correlations between the key metabolite (9.62_838.5595; oxPC38:6+2O) and a clinical parameter are illustrated in a 2D plot. The summary data for panel B is provided in Excel Table S6. Note: AA, amino acid, and analog; cDLCO, carbon monoxide diffusing capacity; FEV1, forced expiratory volume in 1 s; FVC, forced vital capacity; HDLI, humidifier disinfectant–associated lung injury; lysoPC, lysophosphatidylcholine; lysoPE, lysophosphatidylethanolamine; PUFA, polyunsaturated fatty acid.

Phosphatidylcholine (PC) is a primary component of cell membranes, typically comprising ~50% of the total phospholipid mass of most cells and their organelles.[39] oxPC, which is produced through PC oxidation, can compromise the structural integrity and fluidity of cell membranes, adversely affecting membrane function, cell signaling, and overall cellular health.[40] In addition, oxPC acts as a recognizable signal for the immune system known as damage-associated molecular pattern (DAMP).[41] Furthermore, oxPC is a component of oxidized low-density lipoprotein (oxLDL). oxLDL contributes to atherosclerosis by promoting the formation of artery-clogging plaques that increase the risk of cardiovascular events.[42] oxLDL can also trigger inflammation and impair blood vessel function, contributing to various chronic diseases.[43] Previous *in vitro* studies have shown that PHMG-treated cells exhibited increased uptake of oxLDL by macrophages.[44] Consequently, elevated levels of oxPC in HDLI patients suggest a potential risk for developing cardiovascular and chronic inflammatory diseases. Further studies are necessary to analyze plasma levels of oxLDL in HDLI patients and assess their susceptibility to these conditions.

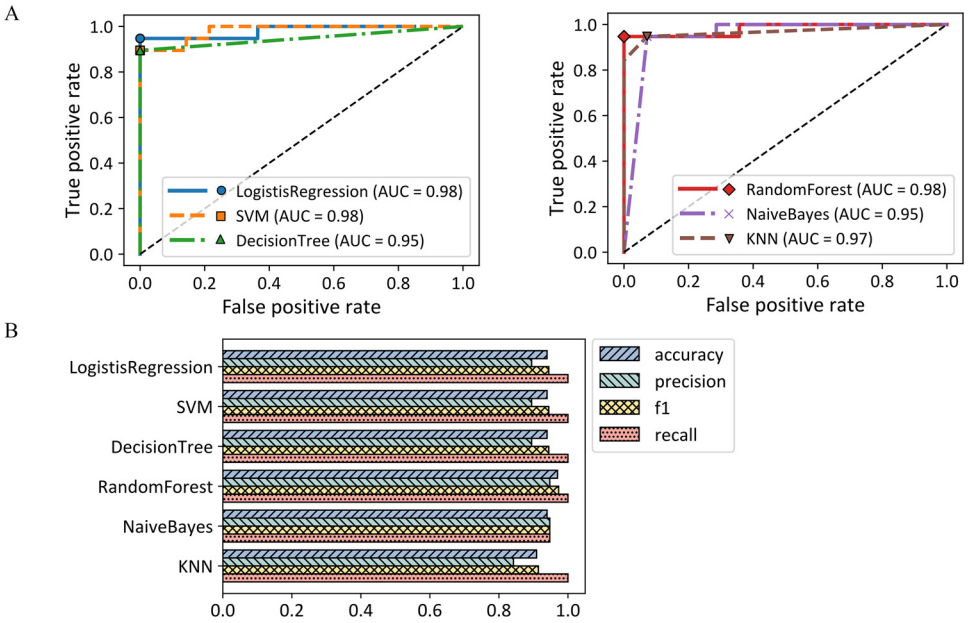

Figure 7. Evaluation of the classification model constructed by ML algorithms. (A) We constructed six machine learning models (logistic regression, SVM, decision tree, random forest, KNN, and naïve Bayes), which were trained on a child training dataset ($n = 74$) with 47 selected key features (key metabolites). A standard scaler was applied to the data prior to training. ROC curve analysis was performed on a test dataset ($n = 33$) to evaluate the models' ability to distinguish HDLI from healthy controls. The Youden index was used to identify the optimal cutoff point in the ROC analysis. (B) We assessed accuracy, precision, recall, and F1 scores for each ML model to compare their performance on the test dataset. The scores for all models are shown in Table S6. Note: HDLI, humidifier disinfectant–associated lung injury; KNN, K-nearest neighbor; ML, machine learning; ROC, receiver operating characteristic; SVM, support vector machines.

This study has several limitations, including a small sample size. Although we validated the key metabolic signatures identified in children with HDLI in an adult population, the limited availability of patients with a "definite" HDLI diagnosis from the physical health monitoring program at the Humidifier Disinfectant Health Center meant that we only managed to recruit 20 patients in the definite group. The mortality rate in this cohort exceeded 40%,[20,45] but we have been tracking the survivors since their injury. To maintain consistency, we also included 20 randomly selected participants in both the unlikely and control groups. In addition, due to the low incidence of BO, we could only recruit seven patients from the Childhood Asthma and Atopy Center at Asan Medical Center. Although the sample size was small, the BO and asthma groups were included to assess the potential link between key metabolites and humidifier disinfectant exposure. The nonuse of humidifier disinfectants in these groups was verified through a questionnaire. The analysis revealed that most key metabolite levels, including oxidized lipids, differed significantly from those in the HDLI group, indicating a possible association between these metabolites and HDLI.

Despite the strong performance of our ML models, which achieved high AUC (>0.95), F1 (>0.91), and precision scores (>0.84) using 47 key metabolites, these results indicate the potential utility of these metabolites rather than confirming their readiness for clinical application. Moreover, although we validated the metabolites in both the child and adult cohorts, larger studies are required to establish the diagnostic specificity of these metabolites and ensure their reliability as HDLI diagnosis biomarkers.[46,47] Nevertheless, the ongoing health monitoring program at the Humidifier Disinfectant Health Center provides a valuable opportunity for future research, potentially tracking changes in the intensity of these key metabolites, which could provide deeper insights into the progression of HDLI and its long-term effects. Follow-up observations will be essential to validate these findings and assess the progression patterns of these metabolites.

Exposure assessment was conducted using questionnaires administered by an environmental health specialist (see Supplemental Material, "Questionnaire"). However, given that this was a retrospective study, inaccuracies might be possible. Although uncertainties remain regarding the precise level of exposure, HDLI diagnosis was not based solely on exposure history. Instead, it incorporated a combination of clinical, pathological, and radiological criteria, providing a more comprehensive diagnostic approach.[20] Clinically, HDLI patients typically exhibited symptoms such as dyspnea, tachypnea, and coughing, with no signs of respiratory infection. Radiological findings varied by disease stage[1]: the early phase showed multifocal patchy consolidation in the subpleural zones of the lower lungs; diffuse centrilobular ground-glass opacities were seen in the subacute phase; and diffuse homogeneous ground-glass opacity with pneumomediastinum were noted in the late phase.

Although quantifying exact exposure levels is challenging, integrating clinical and radiological criteria helps distinguish HDLI from other respiratory diseases. Epidemiological investigations suggest a link between humidifier disinfectant exposure and the disease, based on findings from both pediatric[3,4] and adult cases.[5] The disease primarily affected children and pregnant women during winter outbreaks, and no new cases have been reported since the ban on humidifier disinfectants.[20] Key strength of our study is its focus on identifying metabolic signatures in children, who have lower exposure to environmental factors such as smoking in comparison with adults. This reduced exposure to confounding factors may strengthen the association between the identified metabolic signatures and HDLI.

Another study limitation was the characterization of oxidized lipids, which exhibit structural diversity in forms such as epoxides, hydroxides, hydroperoxides, aldehydes, and carboxylic acids. This diversity may impact the accuracy of lipid identification through LC-MS/MS analysis. Moreover, biases can arise from both the extraction methods employed and the

databases available for metabolite annotation. Different extraction techniques can significantly affect the types and concentrations of metabolites detected,[48] potentially leading to selective detection. In addition, when annotation databases lack relevant information on specific metabolites in the MS/MS datasets, this can result in missing data during the annotation process.[49] Despite these biases potentially affecting data comprehensiveness, this approach enables the identification of a broader range of metabolites in comparison with targeted methods. This expanded scope enhances the discovery of novel metabolites that may play critical roles in biological processes and disease mechanisms, allowing for deeper exploration of metabolic pathways and interactions within complex biological systems.[50]

The HDLI incident was a tragedy that underscored the importance of product safety in South Korea, and the potential risks associated with household chemicals. The incident serves as a reminder of the need for rigorous testing and regulation of consumer products to protect public health and emphasizes the importance of using safe, approved disinfectants and adhering to product usage guidelines. Our study provides crucial insights into the pathogenesis of HDLI by identifying key plasma metabolites, specifically oxidized lipids, which were significantly altered in affected individuals in comparison with controls. These metabolic signatures, validated across different age groups, offer exceptional diagnostic potential for HDLI and highlight a putative mechanism involving ER stress, mitochondrial apoptosis, ROS generation, lipid peroxidation, and inflammation. Moreover, they could facilitate long-term monitoring of HDLI. These findings enhance our understanding and potential biomarkers of HDLI and emphasize the need for stricter regulation of disinfectant products to prevent similar public health disasters. We anticipate that this study could illuminate the unique metabolic signatures associated with HDLI.

Acknowledgments

The authors sincerely appreciate the dedication of health care professionals involved in caring for patients with HDLI at intensive care units. The authors extend their heartfelt condolences to all those who experienced sickness or who lost loved ones due to the use of toxic humidifier disinfectants.

This work was supported by the National Research Foundation of Korea, funded by the Korean government (MIST: RS-2022-NR068424), and by a grant from the National Institute of Environmental Research (NIER), funded by the Ministry of Environment (ME) of the Republic of Korea (NIER-2017-04-02-023).

References

1. Lee E, Seo J-H, Kim HY, Yu J, Jhang W-K, Park S-J, et al. 2013. Toxic inhalational injury-associated interstitial lung disease in children. J Korean Med Sci 28(6):915–923, PMID: 23772158, https://doi.org/10.3346/jkms.2013.28.6.915.
2. Hong S-B, Kim HJ, Huh JW, Do K-H, Jang SJ, Song JS, et al. 2014. A cluster of lung injury associated with home humidifier use: clinical, radiological and pathological description of a new syndrome. Thorax 69(8):694–702, PMID: 24473332, https://doi.org/10.1136/thoraxjnl-2013-204135.
3. Kim KW, Ahn K, Yang HJ, Lee S, Park JD, Kim WK, et al. 2014. Humidifier disinfectant-associated children's interstitial lung disease. Am J Respir Crit Care Med 189(1):48–56, PMID: 24199596, https://doi.org/10.1164/rccm.201306-1088OC.
4. Yang H-J, Kim H-J, Yu J, Lee E, Jung Y-H, Kim H-Y, et al. 2013. Inhalation toxicity of humidifier disinfectants as a risk factor of children's interstitial lung disease in Korea: a case-control study. PLoS One 8(6):e64430, PMID: 23755124, https://doi.org/10.1371/journal.pone.0064430.
5. Kim HJ, Lee M-S, Hong S-B, Huh JW, Do K-H, Jang SJ, et al. 2014. A cluster of lung injury cases associated with home humidifier use: an epidemiological investigation. Thorax 69(8):703–708, PMID: 24488371, https://doi.org/10.1136/thoraxjnl-2013-204132.
6. Lamichhane DK, Leem J-H, Lee S-M, Yang H-J, Kim J, Lee J-H, et al. 2019. Family-based case-control study of exposure to household humidifier disinfectants and risk of idiopathic interstitial pneumonia. PLoS One 14(9):e0221322, PMID: 31487292, https://doi.org/10.1371/journal.pone.0221322.
7. Park J-H, Kim HJ, Kwon G-Y, Gwack J, Park Y-J, Youn S-K, et al. 2016. Humidifier disinfectants are a cause of lung injury among adults in South Korea: a community-based case-control study. PLoS One 11(3):e0151849, PMID: 26990641, https://doi.org/10.1371/journal.pone.0151849.
8. Park D-U, Ryu S-H, Roh H-S, Lee E, Cho H-J, Yoon J, et al. 2018. Association of high-level humidifier disinfectant exposure with lung injury in preschool children. Sci Total Environ 616-617:855–862, PMID: 29126637, https://doi.org/10.1016/j.scitotenv.2017.10.237.
9. Huh JW, Hong SB, Do KH, Koo HJ, Jang SJ, Lee MS, et al. 2016. Inhalation lung injury associated with humidifier disinfectants in adults. J Korean Med Sci 31(12):1857–1862, PMID: 27822921, https://doi.org/10.3346/jkms.2016.31.12.1857.
10. Yoon J, Kang M, Jung J, Ju MJ, Jeong SH, Yang W, et al. 2021. Humidifier disinfectant consumption and humidifier disinfectant-associated lung injury in South Korea: a nationwide population-based study. Int J Environ Res Public Health 18(11):6136, PMID: 34204162, https://doi.org/10.3390/ijerph18116136.
11. Byeon J, Kim H-S, Park M-y, Lee K-M, Hong M-G, Choi Y-y. 2020. An estimation of population at risk of exposure to humidifier disinfectant and associated health effects. J Environ Health Sci 46:457–469, https://doi.org/10.5668/JEHS.2020.46.4.457.
12. Lee J-H, Kim Y-H, Kwon J-H. 2012. Fatal misuse of humidifier disinfectants in Korea: importance of screening risk assessment and implications for management of chemicals in consumer products. Environ Sci Technol 46(5):2498–2500, PMID: 22369507, https://doi.org/10.1021/es300567j.
13. Lee J-H, Kang H-J, Seol H-S, Kim C-K, Yoon S-K, Gwack J, et al. 2013. Refined exposure assessment for three active ingredients of humidifier disinfectants. Environ Engineering Res 18(4):253–257, https://doi.org/10.4491/eer.2013.18.4.253.
14. Song J-H, Ahn J, Park MY, Park J, Lee YM, Myong J-P, et al. 2022. Health effects associated with humidifier disinfectant use: a systematic review for exploration. J Korean Med Sci 37(33):e257, PMID: 35996934, https://doi.org/10.3346/jkms.2022.37.e257.
15. Lee J, Lee H, Jang S, Hong S-H, Kim WJ, Ryu SM, et al. 2019. CMIT/MIT induce apoptosis and inflammation in alveolar epithelial cells through p38/JNK/ERK1/2 signaling pathway. Mol Cell Toxicol 15(1):41–48, https://doi.org/10.1007/s13273-019-0005-0.
16. Park YJ, Jeong MH, Bang IJ, Kim HR, Chung KH. 2019. Guanidine-based disinfectants, polyhexamethylene guanidine-phosphate (PHMG-P), polyhexamethylene biguanide (PHMB), and oligo (2-(2-ethoxy) ethoxyethyl guanidinium chloride (PGH) induced epithelial-mesenchymal transition in A549 alveolar epithelial cells. Inhal Toxicol 31(4):161–166, PMID: 31179775, https://doi.org/10.1080/08958378.2019.1624896.
17. Kim HR, Lee K, Park CW, Song JA, Shin DY, Park YJ, et al. 2016. Polyhexamethylene guanidine phosphate aerosol particles induce pulmonary inflammatory and fibrotic responses. Arch Toxicol 90(3):617–632, PMID: 25716161, https://doi.org/10.1007/s00204-015-1486-9.
18. Kim H, Chung Y, Park Y. 2017. Intra-tracheal administration of the disinfectant chloromethylisothiazolinone/methylisothiazolinone (CMIT/MIT) in a mouse model to evaluate a causal association with death. J Environ Health Sci 43(4):247–256, https://doi.org/10.5668/JEHS.2017.43.4.247.
19. Lee M-S, Kim HJ. 2016. Epidemiologic research on lung damage caused by humidifier disinfectants. Epidemiol Health 38:e2016031, PMID: 27457061, https://doi.org/10.4178/epih.e2016031.
20. Paek D, Koh Y, Park D-U, Cheong H-K, Do K-H, Lim C-M, et al. 2015. Nationwide study of humidifier disinfectant lung injury in South Korea, 1994–2011 incidence and dose-response relationships. Ann Am Thorac Soc 12(12):1813–1821, PMID: 26653190, https://doi.org/10.1513/AnnalsATS.201504-221OC.
21. Kang MJ, Ahn HS, Lee SY, Yeom J, Kim K, Hong SJ. 2022. TGFβ1 and POSTN as biomarkers of postinfectious bronchiolitis obliterans and asthma in children. Pediatr Pulmonol 57(12):3161–3164, PMID: 36175004, https://doi.org/10.1002/ppul.26139.
22. Park JS, Choi YJ, Suh DI, Jung S, Kim Y-H, Lee S-Y, et al. 2019. Profiles and characteristics of bronchial responsiveness in general 7-year-old children. Pediatr Pulmonol 54(6):713–720, PMID: 30859751, https://doi.org/10.1002/ppul.24310.
23. Yang H-J, Lee S-Y, Suh DI, Shin YH, Kim B-J, Seo J-H, et al. 2014. The Cohort for Childhood Origin of Asthma and allergic diseases (COCOA) study: design, rationale and methods. BMC Pulm Med 14:109–112, PMID: 24990471, https://doi.org/10.1186/1471-2466-14-109.
24. Park D-U. 2018. A strategy for exposure assessment of humidifier disinfectant associated to health effects. J Environ Health Sci 44(2):107–114.
25. Park DU, Friesen MC, Roh HS, Choi YY, Ahn JJ, Lim HK, et al. 2015. Estimating retrospective exposure of household humidifier disinfectants. Indoor Air 25(6):631–640, PMID: 25557769, https://doi.org/10.1111/ina.12180.
26. Djoumbou-Feunang Y, Pon A, Karu N, Zheng J, Li C, Arndt D, et al. 2019. CFM-ID 3.0: significantly improved ESI-MS/MS prediction and compound identification. Metabolites 9(4):72, PMID: 31013937, https://doi.org/10.3390/metabo9040072.
27. Wishart DS, Guo A, Oler E, Wang F, Anjum A, Peters H, et al. 2022. HMDB 5.0: the human metabolome database for 2022. Nucleic Acids Res 50(D1):D622–D631, PMID: 34986597, https://doi.org/10.1093/nar/gkab1062.

28. Sumner LW, Amberg A, Barrett D, Beale MH, Beger R, Daykin CA, et al. 2007. Proposed minimum reporting standards for chemical analysis. Metabolomics 3(3):211–221, PMID: 24039616, https://doi.org/10.1007/s11306-007-0082-2.
29. Cho H-J, Lee SY, Park D, Ryu S-H, Yoon J, Jung S, et al. 2019. Early-life exposure to humidifier disinfectant determines the prognosis of lung function in children. BMC Pulm Med 19(1):261, PMID: 31870444, https://doi.org/10.1186/s12890-019-1028-y.
30. Brzezinska MS, Walczak M, Jankiewicz U, Pejchalová M. 2018. Antimicrobial activity of polyhexamethylene guanidine derivatives introduced into polycaprolactone. J Polym Environ 26(2):589–595, https://doi.org/10.1007/s10924-017-0974-9.
31. Song J, Jung KJ, Yoon SJ, Lee K, Kim B. 2019. Polyhexamethyleneguanidine phosphate induces cytotoxicity through disruption of membrane integrity. Toxicology 414:35–44, PMID: 30629986, https://doi.org/10.1016/j.tox.2019.01.001.
32. Ha Y, Kwon JH. 2020. Effects of lipid membrane composition on the distribution of biocidal guanidine oligomer with solid supported lipid membranes. RSC Adv 10(38):22343–22351, PMID: 35514581, https://doi.org/10.1039/d0ra03108a.
33. Jeong MH, Jeon MS, Kim GE, Kim H. 2021. Polyhexamethylene guanidine phosphate induces apoptosis through endoplasmic reticulum stress in lung epithelial cells. Int J Mol Sci 22(3):1215, PMID: 33530568, https://doi.org/10.3390/ijms22031215.
34. Leem JH, Kim H-C. 2020. Mitochondria disease due to humidifier disinfectants: diagnostic criteria and its evidences. Environ Anal Health Toxicol 35(2):e2020007, PMID: 32693559, https://doi.org/10.5620/eaht.e2020007.
35. Su L-J, Zhang J-H, Gomez H, Murugan R, Hong X, Xu D, et al. 2019. Reactive oxygen species-induced lipid peroxidation in apoptosis, autophagy, and ferroptosis. Oxid Med Cell Longev 2019:5080843, PMID: 31737171, https://doi.org/10.1155/2019/5080843.
36. Ayala A, Muñoz MF, Argüelles S. 2014. Lipid peroxidation: production, metabolism, and signaling mechanisms of malondialdehyde and 4-hydroxy-2-nonenal. Oxid Med Cell Longev 2014:360438, PMID: 24999379, https://doi.org/10.1155/2014/360438.
37. Yin H, Xu L, Porter NA. 2011. Free radical lipid peroxidation: mechanisms and analysis. Chem Rev 111(10):5944–5972, PMID: 21861450, https://doi.org/10.1021/cr200084z.
38. Dennis EA, Norris PC. 2015. Eicosanoid storm in infection and inflammation. Nat Rev Immunol 15(8):511–523, PMID: 26139350, https://doi.org/10.1038/nri3859.
39. Testerink N, van der Sanden MHM, Houweling M, Helms JB, Vaandrager AB. 2009. Depletion of phosphatidylcholine affects endoplasmic reticulum morphology and protein traffic at the Golgi complex. J Lipid Res 50(11):2182–2192, PMID: 19458387, https://doi.org/10.1194/jlr.M800660-JLR200.
40. Volinsky R, Kinnunen PK. 2013. Oxidized phosphatidylcholines in membrane-level cellular signaling: from biophysics to physiology and molecular pathology. FEBS J 280(12):2806–2816, PMID: 23506295, https://doi.org/10.1111/febs.12247.
41. Matt U, Sharif O, Martins R, Knapp S. 2015. Accumulating evidence for a role of oxidized phospholipids in infectious diseases. Cell Mol Life Sci 72(6):1059–1071, PMID: 25410378, https://doi.org/10.1007/s00018-014-1780-3.
42. Berliner JA, Leitinger N, Tsimikas S. 2009. The role of oxidized phospholipids in atherosclerosis. J Lipid Res 50(suppl):S207–S212, PMID: 19059906, https://doi.org/10.1194/jlr.R800074-JLR200.
43. Poznyak AV, Nikiforov NG, Markin AM, Kashirskikh DA, Myasoedova VA, Gerasimova EV, et al. 2020. Overview of OxLDL and its impact on cardiovascular health: focus on atherosclerosis. Front Pharmacol 11:613780, PMID: 33510639, https://doi.org/10.3389/fphar.2020.613780.
44. Kim J-Y, Kim HH, Cho K-H. 2013. Acute cardiovascular toxicity of sterilizers, PHMG, and PGH: severe inflammation in human cells and heart failure in zebrafish. Cardiovasc Toxicol 13(2):148–160, PMID: 23225114, https://doi.org/10.1007/s12012-012-9193-8.
45. Lee E, Lee S-Y, Hong S-J. 2020. The past, present and future of humidifier disinfectant-associated interstitial lung diseases in children. Clin Exp Pediatr 63(7):251–258, PMID: 32024320, https://doi.org/10.3345/cep.2019.01326.
46. Liang D, Li Z, Vlaanderen J, Tang Z, Jones DP, Vermeulen R, et al. 2023. A state-of-the-science review on high-resolution metabolomics application in air pollution health research: current progress, analytical challenges, and recommendations for future direction. Environ Health Perspect 131(5):056002, PMID: 37192319, https://doi.org/10.1289/EHP11851.
47. Baccarelli A, Dolinoy DC, Walker CL. 2023. A precision environmental health approach to prevention of human disease. Nat Commun 14(1):2449, PMID: 37117186, https://doi.org/10.1038/s41467-023-37626-2.
48. Hemmer S, Manier SK, Wagmann L, Meyer MR. 2024. Impact of four different extraction methods and three different reconstitution solvents on the untargeted metabolomics analysis of human and rat urine samples. J Chromatogr A 1725:464930, PMID: 38696889, https://doi.org/10.1016/j.chroma.2024.464930.
49. Chaleckis R, Meister I, Zhang P, Wheelock CE. 2019. Challenges, progress and promises of metabolite annotation for LC–MS-based metabolomics. Curr Opin Biotechnol 55:44–50, PMID: 30138778, https://doi.org/10.1016/j.copbio.2018.07.010.
50. Johnson CH, Ivanisevic J, Siuzdak G. 2016. Metabolomics: beyond biomarkers and towards mechanisms. Nat Rev Mol Cell Biol 17(7):451–459, PMID: 26979502, https://doi.org/10.1038/nrm.2016.25.